Lipid bilayers decorated with photosensitive ruthenium complexes

Bahreman, A.

5

Liposomes functionalized with ruthenium complexes: towards tumor targeted light-controlled anticancer prodrugs

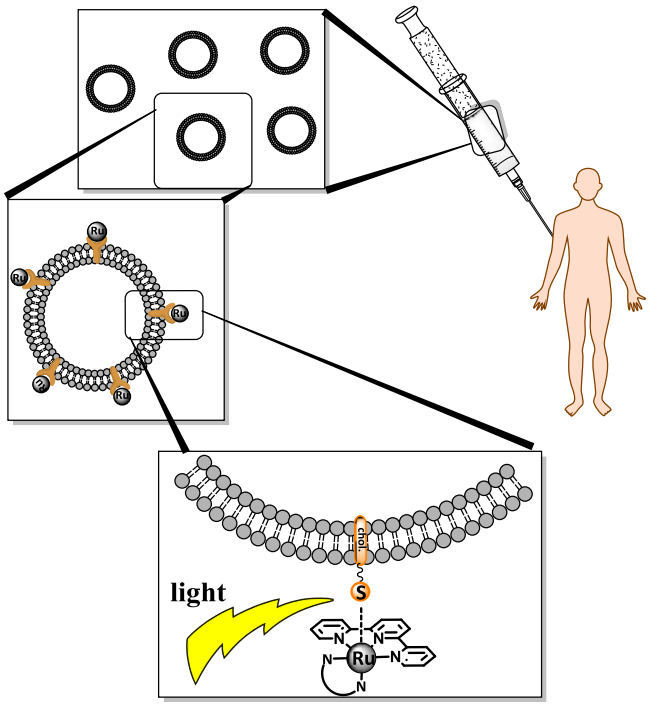

This Chapter will be submitted as a paper;
Bahreman, A.; Van Geest, E.; Heger, M.; Balemans, C.; Lupica Spagnolo, L.; Bonnet, S.; manuscript in preparation

Abstract

Ruthenium complexes [**1**]$(PF_6)_2$ to [**4**]$(PF_6)_2$ with the general formula [Ru(terpy)(N-N)(SRR')]$^{2+}$ were synthesized, where terpy is 2,2';6',2''-terpyridine, N-N is 2,2'-bipyridine (bpy) or phenylpiridin-2-ylmethylene-imine (pymi), and SRR' is a thioether-cholesterol conjugate with a cholesterol tail. Stable DMPC, DMPG, DOPC or DOPG liposomes functionalized with these complexes were prepared by extrusion. The ruthenium complexes supported on liposomes were photosensitive: substitution of the SRR' ligand by an aqua ligand occurred upon blue light irradiation (λ_e=452 nm), thus leading to the detachment of the complex from the liposome surface. Kinetic studies using UV-vis spectroscopy on DOPC and DMPG liposomes decorated with the ruthenium complexes [**1**]$(PF_6)_2$ to [**4**]$(PF_6)_2$ showed that the photoreactivity of these complexes increased at human body temperature as compared to room temperature, or when the liposome is composed of neutral lipids (DOPC) as compared to negatively charged lipids (DMPG). The Ru-S coordination bond of complex [**2**]$(PF_6)_2$ supported on a DOPC liposome in a PBS buffer was shown to be stable in the dark at 4 °C for at least 7 days.

Cancer cells were incubated with Ru-functionalized liposomes to study the influence of liposome formulation on cellular uptake. For HepG2 cells confocal microscope images proved that fluorescently labeled liposomes containing [**1**]$(PF_6)_2$ were better taken up when the lipid composing the membrane was neutral (DMPC) than when it was negatively charged (DMPG). The same effect was observed for the cellular uptake of neutral (DOPC) or negatively charged (DOPG) liposomes functionalized with [**1**]$(PF_6)_2$ by ovarian cancer cells (A2780 and A2780 R). When PEGylated lipids were added in the liposome formulation, the effect of the lipid charge was shielded and no difference in cellular uptake was observed between DOPC- and DOPG-based formulations functionalized with [**1**]$(PF_6)_2$, [**2**]$(PF_6)_2$, [**3**]$(PF_6)_2$, or [**4**]$(PF_6)_2$.

The cytotoxicity of PEGylated liposomes functionalized with complexes [**1**]$(PF_6)_2$ – [**4**]$(PF_6)_2$ in the dark was tested on A2780 and A2780 R ovarian cancer cells. The results show that none of the ruthenium-functionalized liposomes is significantly toxic in the dark after 6 hours incubation time. Light cytotoxicity tests for non-PEGylated DMPC and DMPG liposomes functionalized with [**1**]$(PF_6)_2$ showed up to five times higher cytotoxicity after blue light activation, compared to dark toxicity.

5.1 Introduction

Ruthenium-based compounds have attracted much attention as potential anticancer agents.[1-3] A significant number of the ruthenium complexes studied in this field exert their anticancer activity *via* initial substitution of a ligand by a water molecule.[4] The hydrolyzed ruthenium complex is believed to be cytotoxic by interacting with DNA or other biomolecules in the cancer cells.[5-6] The released ligand might also be biologically active and bind to nucleic acids or protein active sites.[7] Ruthenium complexes often absorb light in the visible region (λ_{max}~450 nm) and their photophysical properties can be tuned. In particular complexes with distorted octahedral geometry may undergo photosubstitution reactions upon visible light irradiation, which can be used in photoactivated chemotherapy (PACT).[8] The great advantage of photoactivation of ruthenium-based prodrugs is to control the time and place of complex activation, which results in a greater selectivity of the cytotoxicity.[9-10] In this case the ground state complex should be thermally stable and not undergo spontaneous ligand exchange or hydrolysis.[11-13]

When developing ruthenium-based cytotoxic compounds efficient drug targeting is also an important issue. Nano-sized drug delivery systems such as nanoparticles, micelles, or liposomes, can be used for specific delivery of the prodrug to cancer cells.[14] Provided that these drug delivery systems stay long enough in the blood circulation, increased accumulation of the prodrug can be obtained at the tumor sites.[15] For example, Sauvage and coworkers[16] recently used mesoporous silica nanoparticles (MSNPs) as drug carriers for photosensitive ruthenium dipyridophenazine (dppz) complexes. The resulting supramolecular assembly showed fast cellular uptake and induced cytotoxic activity upon visible light irradiation.

Liposomal drug carriers have been extensively used in anticancer therapy since 1974.[17-20] In tumor tissues the endothelium (blood vessel wall) is distorted and can be crossed by liposomes. As a result liposomes penetrate well cancer tissues, and less well healthy tissues.[21] It is known that several factors such as liposome size, surface charge, and composition, influence their clearance by cells of the immune system and thus their circulations lifetime in the blood stream.[22-25] For example liposomes with small sizes (<200 nm), with cholesterol in the membrane composition, and a high phase transition temperature, show a longer biological half-life.[26-28] In particular, adding poly(ethylene glycol) (PEG)-functionalized lipids in the composition of the

liposomes was reported to be the most successful method to increase the blood circulation lifetime of liposomes. The hydrophobic PEG groups protect the liposome surface and prevent its clearance by cells of the immune system.[29-30] Although several formulations are now clinically tested with organic drugs, liposomal drug carriers have not often been used for metal-based drugs,[31-33] and the first liposomal system for an anticancer ruthenium(III) complexes was reported only recently by Paduana and co-workers.[34-35] To the best of our knowledge liposomes have not yet been used for the delivery of light-activatable ruthenium complexes.

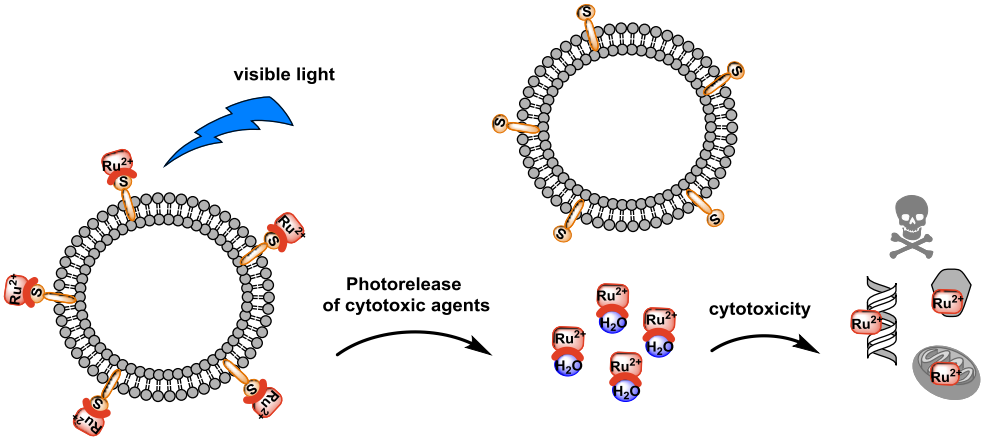

Scheme 5.1. Schematic drawing of a liposome functionalized with photosensitive ruthenium complexes. Photosubstitution of membrane-embedded sulfur ligands by aqua ligands releases ruthenium-aqua complexes, which may be cytotoxic by interacting with DNA, mitochondria, or other biomolecules.

In Chapters 2 and 3 polypyridyl ruthenium complexes of the type $[Ru(terpy)(N\text{-}N)(SRR')]^{2+}$ were described, where terpy is 2,2′;6′,2″-terpyridine, N-N is a diimine ligand, and SRR' is a sulfur-containing ligand. These complexes undergo selective photosubstitution of the SRR' ligand by an aqua ligand upon visible light irradiation. In addition it was shown in Chapter 3 that for less distorted complexes (*e.g.*, N-N=2,2'-bipyridine) the Ru-S bond is rather stable in the dark below 50 °C. Thus, these complexes are potentially interesting as light-activatable anticancer agents, if the corresponding aqua complex is cytotoxic. Moreover, a strategy to decorate liposomes with these photosensitive ruthenium complexes was recently published in our group;[36] such a supramolecular assembly may deliver the ruthenium complex to cancer cells. Provided the Ru-functionalized liposomes are taken up by cancer cells, light-induced

substitution of a membrane-bound sulfur ligand by an aqua ligand would result in the dissociation of the ruthenium aqua complex from the liposome carrier, followed by the diffusion of the complex into the cell, its interaction with biomolecules, and possibly to cell death (see Scheme 5.1). In this Chapter the preparation, characterization, and biological activity are described of liposomes functionalized with a photoactive ruthenium complex (see Figure 5.1).

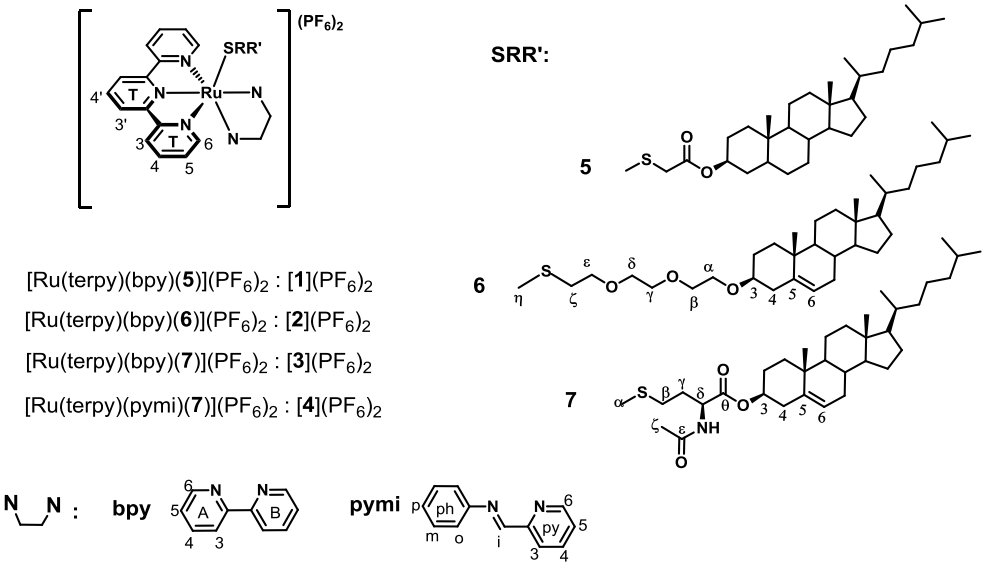

Figure 5.1. Chemical structures and numbering scheme of polypyridyl ruthenium complexes [**1**]$(PF_6)_2$ – [**4**]$(PF_6)_2$.

5.2 Results

5.2.1. Synthesis

The synthesis of ligands **5**[36] and **6** (Chapter 2, Appendix II) is reported elsewhere. Ligand **7** was synthesized following a modified literature procedure,[37] consisting in the esterification of cholesterol with N-acetylated methionine using DCC (dicyclohexylcarboiimide) as coupling reagent and DMAP (N,N-dimethylaminopyridine) as catalyst. The sulfur-sterol conjugates **6** and **7** were

coordinated to ruthenium following the procedure reported for complex [**1**]$(PF_6)_2$, by the reaction of [Ru(terpy)(bpy)(Cl)]Cl or [Ru(terpy)(pymi)(Cl)]Cl with **6** or **7** in the presence of two equiv. of $AgBF_4$ in acetone, followed by column chromatography.[36] Complexes [Ru(terpy)(bpy)(**6**)]$(PF_6)_2$ ([**2**]$(PF_6)_2$), [Ru(terpy)(bpy)(**7**)]$(PF_6)_2$ ([**3**]$(PF_6)_2$), and [Ru(terpy)(pymi)(**7**)]$(PF_6)_2$ ([**4**]$(PF_6)_2$) were obtained as orange, water-insoluble powders. They were characterized by ^{1}H NMR, ^{13}C NMR, mass spectrometry, UV-vis spectroscopy, and elemental analysis.

5.2.2. Photoreactivity and dark stability of a Ru-S bond at liposomes

5.2.2.1. Visible light irradiation of Ru-decorated liposome samples

In order to study the photosubstitution kinetics for complexes [**1**]$(PF_6)_2$, [**2**]$(PF_6)_2$, [**3**]$(PF_6)_2$, or [**4**]$(PF_6)_2$ at a lipid bilayer surface, liposomes composed of 1,2-dioleoyl-*sn*-glycero-3-phosphocholine (hereafter DOPC) or 1,2-dimyristoyl-*sn*-glycero-3-phospho-(1'-rac-glycerol) sodium salt (hereafter DMPG) functionalized with 5 mol% of one of the ruthenium complexes were prepared a in phosphate buffer (I=50 mM, pH=7.0) (Table 5.1). Each liposome sample was characterized by DLS prior to performing other experiments; their average diameter was 130-140 nm. The photosubstitution of the sulfur-sterol conjugate **5**, **6**, or **7** by an aqua ligand upon irradiation with blue light (λ_e=452 nm) was investigated by UV-vis spectroscopy either at 25 °C or at 37 °C. For a typical experiment the liposome sample was irradiated from the top of the UV-vis cuvette, while UV-vis spectra were measured perpendicular to the irradiating light beam (see Appendix I, Figure AI.1). The absorption spectrum of the irradiated sample gradually evolved until a photochemical steady state was obtained, characterized by an absorption maximum at a longer wavelength. In each case an isosbestic point was observed, which indicated that a single photochemical reaction was taking place. The UV-vis spectrum at the photochemical steady state corresponded with that of the ruthenium-aqua species $[Ru(terpy)(N\text{-}N)(OH_2)]^{2+}$ (N-N=bpy or pymi). The concentration of the ruthenium-sulfur complex (RuSRR') was calculated in each experiment as a function of irradiation time (see Appendix I, section AI.2.1). As shown in Equation 5.1, the photosubstitution first-order rate constants k_φ was obtained from the slope of a plot of $\ln([RuSRR']/[Ru]_{tot})$ *vs.* irradiation time (Figure 5.2a), where $[RuSRR']$ and $[Ru]_{tot}$ represent the bulk concentration in RuSRR' and the total ruthenium concentration in the sample, respectively. Half-reaction times were also calculated using Equation 5.2.

$$-\frac{d[RuSRR']}{dt} = \frac{d[RuOH_2]}{dt} = k_\varphi \cdot [RuSRR'] \quad \textbf{(Equation 5.1)}$$

$$t_{1/2} = \frac{ln2}{k_\varphi} \quad \textbf{(Equation 5.2)}$$

The photosubstitution quantum yield φ was obtained from the slope of a plot of the number of moles of RuSRR' remaining in solution, $n_{RuSRR'}$, *vs.* the number of moles of photons Q absorbed by the RuSRR' species since t=0 (see Figure 5.2b and Appendix I, section AI.3.2). The photosubstitution reactivity ($\xi=\varphi\cdot\varepsilon^{\lambda e}$) of the ruthenium complex, where $\varepsilon^{\lambda e}$ is the extinction coefficient of RuSRR' at the irradiation wavelength, better represents the photoreactivity of a complex in a given irradiation condition, and was calculated as well (see Chapter 6). All photochemical data are reported in Table 5.1.

Table 5.1. Data for the photosubstitution of the thioether-sterol conjugate **5**, **6**, or **7** by water for liposomes functionalized with ruthenium complexes [**1**]$(PF_6)_2$, [**2**]$(PF_6)_2$, [**3**]$(PF_6)_2$, or [**4**]$(PF_6)_2$. Irradiation conditions: λ_e = 452 nm, photon flux Φ_{452} = 3.0(8)×10^{-9} Einstein·s^{-1}, irradiation pathlength = 3 cm. Lipid bulk concentration=1.3 mM (as liposomes), total ruthenium concentration $[Ru]_{tot}$ = 0.065 mM, phosphate buffer pH=7.0, I=50 mM.

Ru complex (5 mol%)	**Liposome**	T (°C)	$\varepsilon^{\lambda e}$ ($M^{-1}\cdot cm^{-1}$)	$t_{1/2}$ (min)	k_φ (s^{-1})	φ	ξ ($\varphi\cdot\varepsilon^{\lambda e}$)	$\lambda_{isosb.}$ (nm)
[**1**]$(PF_6)_2$	DOPC	37	6700	21(2)	5.2(3)×10^{-4}	0.019(5)	127(8)	455
[**2**]$(PF_6)_2$	DOPC	37	6800	53(3)	2.2(2)×10^{-4}	0.013(3)	88(6)	455
[**3**]$(PF_6)_2$	DOPC	37	6700	47(3)	2.5(2)×10^{-4}	0.012(4)	80(5)	453
[**4**]$(PF_6)_2$	DOPC	37	5400	95(5)	1.2(3)×10^{-4}	0.0080(5)	43(3)	479
[**3**]$(PF_6)_2$	DOPC	25	6700	90(5)	1.3(2)×10^{-4}	0.0068(5)	46(3)	453
[**3**]$(PF_6)_2$	DMPG	25	5900	156(8)	7.4(5)×10^{-5}	0.0048(4)	28(2)	464
[**4**]$(PF_6)_2$	DOPC	25	5400	135(8)	8.6(7)×10^{-5}	0.0049(4)	26(2)	479
[**4**]$(PF_6)_2$	DMPG	25	4600	325(9)	3.6(3)×10^{-5}	0.0031(6)	14(1)	483

The effect of temperature on the photosubstitution reactivity of complexes [**3**]$(PF_6)_2$ and [**4**]$(PF_6)_2$ was investigated first. The photochemical data for these complexes (Table 5.1) show that the photosubstitution rate and quantum yield are almost twice higher at 37 °C than at 25 °C. Most probably, it is the dependence of the quantum yield φ with temperature that explains the faster reaction at human body temperature. The

transition from the photochemically generated ^{3}MLCT state to the ^{3}MC state leading to ligand substitution is a thermally activated process, which explains why the elevated temperature of the human body is an advantage on the point of view of photoactivation of polypyridyl ruthenium complexes.

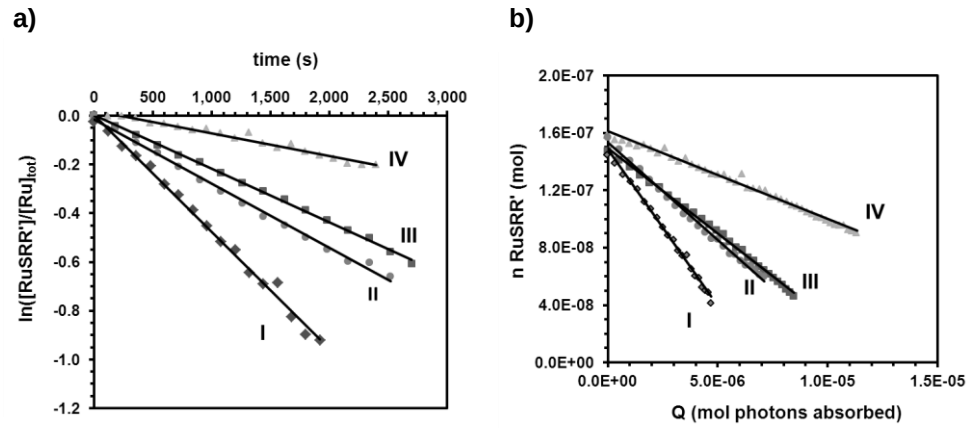

Figure 5.2. a) Plots of ln*([RuSRR']/[Ru]$_{tot}$) vs.* irradiation time during the blue light irradiation of liposomes functionalized with ruthenium complexes [**1**](PF$_6$)$_2$, [**2**](PF$_6$)$_2$, [**3**](PF$_6$)$_2$, or [**4**](PF$_6$)$_2$. *[RuSRR']* represents the bulk concentration in *RuSRR'*, and *[Ru]$_{tot}$* the total ruthenium concentration in the solution. The slope of each plot is $-k_\varphi$ (s^{-1}). (b) Plots of the number of moles of RuSRR' *vs.* the number of moles of photons absorbed by RuSRR' at time *t*, since *t*=0; the slope is the photosubstitution quantum yield φ. RuSRR'=[**1**](PF$_6$)$_2$ (I), [**2**](PF$_6$)$_2$ (II), [**3**](PF$_6$)$_2$ (III), [**4**](PF$_6$)$_2$ (IV). Total ruthenium concentration=0.065 mM, bulk lipid concentration=1.3 mM (as liposomes), phosphate buffer (pH=7, *I*=50 mM). Irradiation condition: blue light (λ_e=452 nm), photon flux Φ_{452}=3.0(8)×10^{-9} Einstein.s^{-1}, *T*=37 °C, irradiation pathlength=3 cm.

Comparing the photosubstitution reactivity of [**1**](PF$_6$)$_2$ – [**4**](PF$_6$)$_2$ on DOPC liposomes at 37 °C shows that the highest quantum yield φ and photosubstitution reactivity value ξ were obtained for complex [**1**](PF$_6$)$_2$, and the lowest for complex [**4**](PF$_6$)$_2$. The higher quantum yield of [**1**](PF$_6$)$_2$ may be due to the higher steric hindrance of the thioether ligand **5**, as the linker between the sulfur atom and the cholesterol moiety is very short. The sulfur ligand is also close to an electron-withdrawing ester, which might exert reductive effects and modify the ability of the ligand to coordinate to the ruthenium. In [**2**](PF$_6$)$_2$ and [**3**](PF$_6$)$_2$ the thioether ligands are electronically similar, leading to similar quantum yields. For [**4**](PF$_6$)$_2$ the non-conjugated imine ligand of the ligand pymi leads to an absorption maximum at higher

wavelength (475 *vs*. 460 nm), thus to a more stable ^{3}MLCT state and (in the absence of steric hindrance) to a lower quantum yield, compared to the bpy-containing complex [**3**]$(PF_6)_2$. Overall, for a given light intensity the time necessary to activate 50% of the complex slightly depends on the chemical structure of the thioether and bidentate ligands.

Another phenomenon was noticed when comparing the photochemical reactivity of two of the four complexes on neutral (DOPC) or negatively charged (DMPG) liposomes at 25 °C. For complex [**3**]$(PF_6)_2$ and [**4**]$(PF_6)_2$ the photosubstitution reactivity ξ and quantum yield φ were found to be about 1.7 and 1.5 times higher, respectively, for DOPC liposomes compared with DMPG liposomes. This observation indicates a non-negligible contribution of the electrostatic interaction between the positively charged ruthenium complex and the negative surface charge of DMPG liposomes, to the strength of the Ru-S bond.

Overall, changing the temperature, the electronic or steric properties of the ligands, or the surface charge of the liposome, all contribute to influencing the photosubstitution quantum yield and reaction rate of the ruthenium complexes upon irradiation.

5.2.2.2. Ruthenium-sulfur bond stability in PBS buffer in the dark

For phototherapy applications the Ru-S bond of Ru-functionalized liposomes as described above is expected to remain stable in the dark and *in vitro*, *i.e.*, the sulfur ligand should not be substituted by water or other ligands (in particular Cl^-) present in biocompatible buffers. Thus, prior to *in vitro* experiments the thermal stability of the Ru-S bond was investigated for complex [**2**]$(PF_6)_2$ supported on PEGylated DOPC liposomes in a PBS (Phosphate Buffered Saline) buffer containing high chloride concentrations (~140 mM). A DOPC:DSPE-PEG2K (98:2) liposome sample (DSPE-PEG2K=1,2-distearoyl-*sn*-glycero-3-phosphoethanolamine-N-[amino(polyethylene glycol)-2000] as the ammonium salt) containing 5 mol% of [**2**]$(PF_6)_2$ was prepared by extrusion. The sample was stored in the refrigerator (4 °C) during one week, and fractions of the sample were subjected to ultracentrifugation (40,000 rpm; 1 h; T = 25 °C) at day 0, 1, 3 and 7. In all cases the lipid pellet obtained after centrifugation was orange and the supernatant was colorless, which qualitatively meant that most of the ruthenium complex was still attached to the lipid bilayer. The ruthenium concentration of the samples before and after centrifugation was quantitatively measured using inductively coupled plasma optical emission spectroscopy (ICP-OES). In all cases (t=0,

1, 3 and 7 days) the total Ru concentration in the supernatant was found to be ~5% (~230 ppb) of the ruthenium concentration found before centrifugation (4170(40) ppb, at *t*=0). These results showed that no ruthenium complex dissociated from the liposome surface after 7 days in such conditions, and that the 5% already present at *t*=0, *i.e.*, just after preparation, were probably produced during extrusion of the sample, which occurs at elevated temperatures (50 °C). Thus, the ruthenium-sulfur bond of complex [**2**]$(PF_6)_2$ supported on DOPC stealth liposomes was found to be stable in the dark in PBS and in the fridge, and the sulfur ligand was not substituted by chloride or water in such conditions.

5.2.3. In vitro experiments

5.2.3.1. Cellular uptake of fluorescently-labeled, Ru-functionalized liposomes

The role of a drug delivery system is to deliver the prodrug inside the target cell, hence the cellular uptake of Ru-functionalized liposomes was investigated first. Liver hepatocellular carcinoma cells (HepG2), non-cisplatin resistant human ovarian cancer cells (A2780), and cisplatin-resistant human ovarian cancer cells (A2780 R), were chosen for *in vitro* experiments. The liposome formulation comprised a phospholipid (DMPC, DMPG, DOPC, or DOPG), 4 – 5 mol% of the fluorescent lipid 1-acyl-2-{12-[(7-nitro-2-1,3-benzoxadiazol-4-yl)amino]dodecanoyl}-*sn*-glycero-3-phosphocholine (hereafter NBD-PC, λ_{exc}=460 nm, λ_{em}=534 nm), 5 mol% of one of the four ruthenium complexes [**1**]$(PF_6)_2$ – [**4**]$(PF_6)_2$, and in some cases 4 mol% of DSPE-PEG2K. All liposomes were prepared by extrusion using a 200 nm polycarbonate filter, resulting in size distributions around 130-150 nm. The cancer cells were incubated with the liposomes for 1 hour, after which the cellular uptake was determined based on the fluorescence of the NBD-PC lipid.

The effect of lipid charge on cellular uptake by HepG2 cells was first investigated for complex [**1**]$(PF_6)_2$ supported on negatively charged (DMPG) or zwitterionic 1,2-dimyristoyl-*sn*-glycero-3-phosphocholine (DMPC) liposomes. Confocal microscopy images were taken after cellular incubation with the liposomes (Figure 5.3). Although Ru-free DMPC liposomes were poorly taken up, Ru-functionalization led to an increased uptake by HepG2 cells. For DMPG liposomes the reverse effect was observed: Ru-free liposomes were well taken up, whereas Ru-functionalized liposomes were less taken up. Thus, the surface charge of the liposome has a critical influence on liposome uptake for HepG2 cells. Overall, for HepG2 cells using neutral lipids in the

liposome formulation seems more beneficial in terms of cellular uptake than using negative lipids.

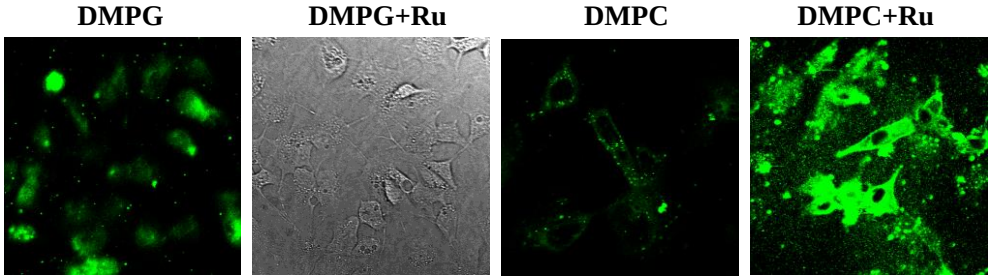

Figure 5.3. Confocal microscope images after cellular uptake of liposomes by HepG2 cells. Intense green color represents higher cellular uptake. Liposome compositions: DMPG:NBD-PC (95:5) and 0 or 5 mol% [**1**]$(PF_6)_2$ or DMPC:NBD-PC (95:5) and 0 or 5 mol% [**1**]$(PF_6)_2$. $[Ru]_{tot}$ = 0.025 mM, $[lipid]_{tot}$=0.50 mM (as liposomes, diameter~140 nm), detection by fluorescence: λ_{ex}=460 nm, λ_{em}=534 nm.

Confocal microscopy images do not provide quantitative information on the cellular uptake of fluorescently-labeled liposomes. As mentioned in section 5.1, liposomes with PEGylated lipids ("stealth" liposomes) are known to have higher blood circulation lifetime than non-PEGylated ones. Thus, cellular uptake experiments were realized using PEGylated Ru-functionalized liposomes and either neutral (DOPC) or negatively charged lipids (1,2-dioleoyl-*sn*-glycero-3-phospho-(1'-rac-glycerol) sodium salt, hereafter DOPG). The lipid formulations consisted in DOPC:DSPE-PEG2K:NBD-PC 92:4:4 or DOPG:DSPE-PEG2K:NBD-PC 92:4:4 mixtures containing no or an additional 5 mol% of one of the four ruthenium complexes [**1**]$(PF_6)_2$ – [**4**]$(PF_6)_2$. The liposomes were prepared by extrusion and characterized by DLS (average diameter ~140 nm). Their ability to enter cancer cells was measured on A2780 and A2780 R cancer cell lines. After 1 hour incubation in the dark the fluorescence of the cell plate was measured at 534 nm (λ_{exc}=460 nm, λ_{em}=534 nm). The fluorescence values F were then corrected for the number of cells by dividing F by the protein content A_{prot} of each well (after lysis), as determined by the BCA (bicinchoninic acid) assay. This protein assay is based on the reduction of Cu^{2+} to Cu^{+} by proteins in an alkaline medium (the biuret reaction); the Cu^{+} subsequently reacts with bicinchoninic acid to form a highly colored (purple) reaction product.[38] The absorption A_{prot} of the reaction product was measured at 562 nm and correlates linearly to the protein concentration of the sample.

Finally the corrected fluorescence value F/A_{prot} of each well was compared to that of untreated cells ($(F/A_{prot})_{ctrl}$=1 or 100%). The results of these cellular uptake experiments are shown in Figure 5.4a.

In both cell lines PEGylated DOPG liposomes without ruthenium were taken up slightly better than PEGylated DOPC liposomes without ruthenium. No significant difference was observed between the different cell lines. For liposomes with ruthenium, uptake of PEGylated DOPG liposomes was comparable with that of PEGylated DOPC liposomes. Although several parameters had changed compared to the uptake experiment on HepG2 cells (Figure 5.2), these new data suggest that the charge of liposomes may be shielded by the PEG groups. Finally, there were no significant differences found for the uptake of PEGylated liposomes functionalized with the different ruthenium complexes [**1**]$(PF_6)_2$ – [**4**]$(PF_6)_2$, which suggests that once supported on liposomes, the exact structure of the complex is of minor importance regarding cellular uptake.

According to these data the uptake of liposomes with ruthenium seemed to be lower than that of liposomes without ruthenium. However, since uptake data were based on the fluorescence intensity of an NBD-PC lipid incorporated in the membrane, the presence of the ruthenium complex at the liposome surface might affect the uptake data, as it might influence (for example by quenching) the fluorescence of the NBD dye. In addition, both the NBD-PC lipid and the ruthenium complex have absorbance maxima around 450-460 nm, and the presence of the Ru complex in the sample might filter the excitation of the NBD dye, leading to artificially lower emission intensities. The effect of the presence of the ruthenium complex at the membrane on NBD-PC emission was checked for different concentrations of complex [**1**]$(PF_6)_2$ in PEGylated DOPC liposomes (DOPC:DSPE-PEG2K:NBD-PC(92:4:4)) (Appendix V, Figure AV.1). In PBS buffer the emission of NBD-PC in the liposome membrane indeed was found to depend on the amount of ruthenium present in the same membrane. With 5 mol% ruthenium the fluorescence intensity was decreased by more than 80%, compared to the emission of a similar liposome without ruthenium. Thus, based on this quenching factor the raw uptake data for DOPC stealth liposomes functionalized with [**1**]$(PF_6)_2$ were corrected (Figure 5.4b). According to this correction, the uptake of liposomes functionalized with complex [**1**]$(PF_6)_2$ was found to be much higher, in both cell lines, than that of Ru-free DOPC liposomes (22.6 *vs.* 3.6 for A2780 cells, and 22.5 *vs.* 3.1 for A2780 R cells). These results are consistent with the conclusions drawn

from confocal microscopy images measured with HepG2 cells, that the presence of Ru complexes at the surface of neutral liposomes enhances liposome uptake.

Because of the fluorescence-quenching problem the uptake results shown in Figure 5.3a do not provide quantitative information about the amount of ruthenium complex taken up by the cells. In an attempt to better quantify ruthenium uptake the cells were lysed using NaOH and the ruthenium concentration in the cell lysis was measured by ICP-OES (see Appendix V). Unfortunately, the concentration of ruthenium in most of the samples was too low to be detected by ICP-OES (*[Ru]* ≤ 20 ppb).

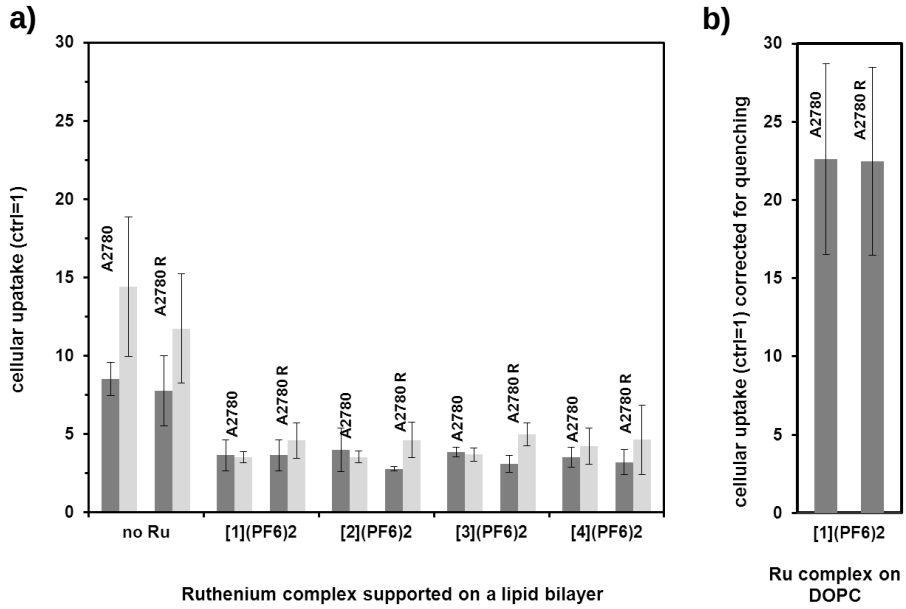

Figure 5.4. a) Cellular uptake of DOPC (dark grey) and DOPG (light grey) stealth (4% PEG) liposomes containing 5 mol% RuSRR' by A2780 and A2780 R human ovarian cancer cells. (b) Uptake data corrected for NBD fluorescence quenching by ruthenium for DOPC stealth liposomes containing 5 mol% of complex [**1**]$(PF_6)_2$. Incubation conditions: bulk lipid concentration $[lipid]_{tot}$= 1.5 mM (as liposomes) in PBS:DMEM (−FCS, +PS, +ph. red) 8:5 medium, total ruthenium concentration $[Ru]_{tot}$ = 0.075 mM, incubation time =1 h, T = 310 K, 7% CO_2, in the dark. Control wells contained untreated cells.

In order to investigate how cellular uptake was influenced by PEG groups at the liposome surface and by the lipid charge, uptake experiments were performed on A2780 and A2780R cells for PEGylated and non-PEGylated liposomes containing

[**1**]$(PF_6)_2$. The fluorescent liposomes were composed of neutral (DOPC) or negatively charged (DOPG) lipids, 0 or 4 mol% DSPE-PEG2K and also an additional 5 mol% [**1**]$(PF_6)_2$. All liposomes were prepared by extrusion in PBS buffer and characterized by DLS (diameter~140 nm) prior to incubation with the cells.

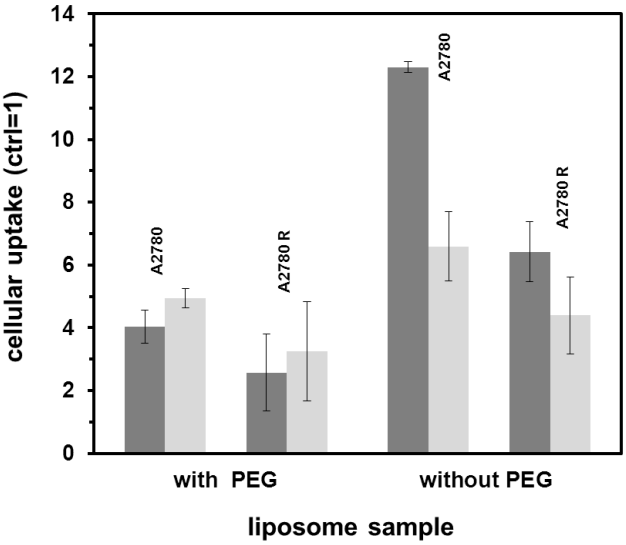

Figure 5.5. Effect of PEGylation on cellular uptake by A2780 or A2780 R human ovarian cancer cells of DOPC (dark grey) and DOPG (light grey) liposomes containing 5 mol% [**1**]$(PF_6)_2$. Liposome formulations: DOPC:DSPE-PEG2K:NBD-PC (92:4:4), DOPG:DSPE-PEG2K:NBD-PC (92:4:4), DOPC: NBD-PC (96:4), or DOPG: NBD-PC (96:4). Incubation conditions: bulk lipid concentration = 1.5 mM (as liposomes) in PBS:DMEM (−FCS, +PS, +ph. red) 8:5, bulk ruthenium concentration $[Ru]_{tot}$ = 0.075 mM, exposure time = 1 h, T = 310 K, 7% CO_2, in the dark. Control wells contained untreated cells.

The uptake data (see Figure 5.5) show that for both cell lines the uptake of non-PEGylated DOPC liposomes was more than twice higher than that of PEGylated liposomes. Assuming that the effect of PEGylation on the fluorescence quenching is negligible, PEGylation thus significantly decreases the uptake of neutral liposomes. Moreover, the decrease in cellular uptake of PEGylated liposomes was more distinct for DOPC liposomes in A2780 cells than in A2780R cells. For negatively charged DOPG liposomes, uptake of PEGylated liposomes was only slightly lower than that of non-PEGylated liposomes in both cell lines. For non-PEGylated liposomes DOPC liposomes were taken up in higher amounts than DOPG liposomes in both cell lines.

This observation is in agreement with the results obtained for HepG2 cells; the difference in uptake can be assigned to the higher influence of positive charges of the ruthenium complexes at the surface of neutral DOPC liposomes, compared to that of the same dicationic complexes at the surface of negatively charged DOPG liposomes. Overall, cellular uptake decreases upon PEGylation, and positive ruthenium complexes at the liposome surface increase the cellular uptake of ruthenium functionalized liposomes in absence of PEGylation.

5.2.3.2. Cytotoxicity

In photoactivated chemotherapy the aim is to activate the anticancer complex using light irradiation. Ideally, liposomes functionalized with ruthenium complexes should be non-toxic (or less toxic) in the dark. The dark cytotoxicity of DOPC or DOPG PEGylated liposomes functionalized with ruthenium complexes was determined for A2780 and A2780 R cell lines. Each formulation consisted of DOPC:DSPE-PEG2K (96:4) or DOPG:DSPE-PEG2K (96:4) mixtures containing 0 or 5 mol% of one of the ruthenium complexes [**1**]$(PF_6)_2$ – [**4**]$(PF_6)_2$. Dark cytotoxicity was determined after 6 h liposome exposure. After incubation the liposomes were removed and cells were incubated in drug-free cell culture medium for 24 h. Then the metabolic activity of the cells was determined using the WST-1 cell proliferation reagent.[39] In this protocol a known quantity of the WST-1 reagent is added to each well, the cells are incubated, and the absorbance W is measured at 450 nm. The formation of a formazan dye is correlated to the metabolic activity of the cells, which can be measured and compared to reference cells. In order to differentiate a large number of poorly active cells from a small number of highly active cells, the metabolic activity obtained by the WST-1 assay was corrected for the amount of cells in each well by dividing the absorbance values W by the protein content A_{prot} of each well as determined in a BCA assay. In order to discuss cell survival, the obtained W/A_{prot} values (corrected metabolic activity) were compared to the corresponding value for untreated cells $(W/A_{prot})_{ctrl}$ =1 or 100%).

The dark cytotoxicity data (Figure 5.6) show that all PEGylated liposomes, with or without ruthenium, exhibited comparably low toxicity against A2780 and A2780 R cells, with cell survival of 70% and 100%, respectively. Thus, no difference was observed between the four different ruthenium complexes and the liposomes were only slightly toxic to A2780 cells and not toxic to A2780 R cells. A low toxicity was observed for A2780 cells treated with liposomes without ruthenium, which suggests

that the toxicity observed in presence of the Ru complex is not due to the metal complexes but to the liposome support. In presence of PEG groups the toxicity of the liposomes was not influenced by the lipid charge (DOPC *vs.* DOPG) in both cell lines.

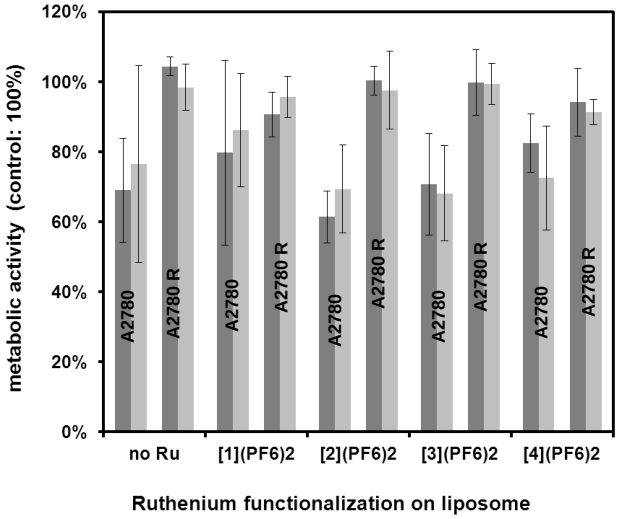

Figure 5.6. Metabolic activity (W/A_{pro}) of A2780 and A2780 R cells exposed to DOPC (dark grey) and DOPG (light grey) stealth liposomes (4 mol% DSPE-PEG2K) with 5 mol% of ruthenium complexes. Metabolic activity of untreated cells (control) is 100%. Conditions: bulk lipid concentration = 1.5 mM (as liposomes) in PBS:DMEM (−FCS, +PS, −ph. red) (8:5), bulk ruthenium concentration $[Ru]_{tot}$ = 0.075 mM, drug exposure time = 6 h, T = 310 K, 7% CO_2, in the dark.

Light cytotoxicity experiments were performed on HepG2 cells exposed to neutral (DMPC) or negatively charged (DMPG) liposomes containing 0 or 5 mol% of complex [**1**]$(PF_6)_2$. Cells were exposed to the liposomes for 30 min, and after removing the liposome solutions each well was irradiated with blue light (λ_e=452 nm, power: 69 mW) for 15 min at 37 °C. The metabolic activity of the cells was measured after 24 h incubation in drug-free medium in the dark using the WST-1 assay as explained above. A control cytotoxicity experiment was also performed in the dark to evaluate the effect of light irradiation with HepG2 cells. As shown in Figure 5.7 for all liposome samples, *i.e.*, with or without ruthenium, cell survival was lower after light exposure compared to non-irradiated cells. The best phototoxic activity was obtained for DMPC liposomes functionalized with [**1**]$(PF_6)_2$, as light cytotoxicity was found to be about 5 times

higher than dark toxicity. For DMPG liposomes with or without ruthenium light cytotoxicity was found to be about 1.6 times higher than dark cytotoxicity.

After irradiation, the metabolic activity of cells treated with DMPC liposomes containing [**1**]$(PF_6)_2$ was lower than that of cells treated with DMPC liposomes without ruthenium. This might be related to the photoactivation of the ruthenium complex [**1**]$(PF_6)_2$ and releasing the corresponding ruthenium aqua complex inside the cells. In the case of DMPG liposomes the metabolic activity with and without ruthenium was almost the same after light exposure. For DMPG liposomes deprived of ruthenium this may be explained by the absence of light-sensitive element in the liposomes formulation, and the lower metabolic activity might simply be the result of the action of blue light on the cells. For Ru-functionalized DMPG liposomes the uptake was low (Figure 5.3), explaining the limited effect of Ru on phototoxicity.

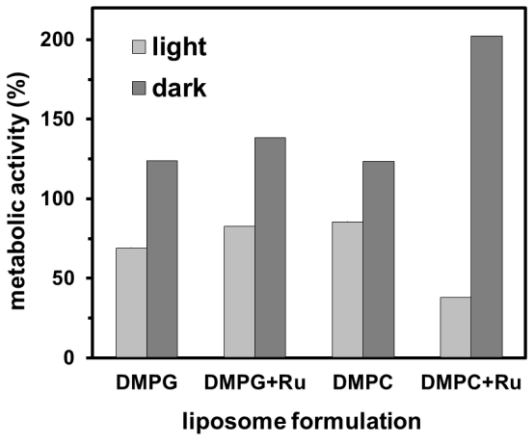

Figure 5.7. Metabolic activity W/A_{prot} (see text) of HepG2 cells exposed to non-PEGylated DMPC or DMPG liposomes containing 0 or 5 mol% [**1**]$(PF_6)_2$ irradiated with blue light (light grey bars) or kept in the dark (dark gray bars); metabolic activity of untreated cells (control) is 100%. DMPG+Ru or DMPC+Ru represent DMPC or DMPG liposomes containing 5 mol % [**1**]$(PF_6)_2$. Conditions: bulk lipid concentration = 2 mM (as liposomes) in phosphate buffer (I=50 mM):PBS: (2:3), bulk ruthenium concentration $[Ru]_{tot}$ = 0.1 mM, drug exposure time = 30 min, T = 37 °C, 7% CO_2. Irradiation parameters: λ_e=452 nm (blue light), light power=69 mW, incident spot diameter = 2.3 cm, light intensity: 17 mW.cm^{-2}.

5.3 Discussion

The uptake data disclosed herein allow for concluding about an optimal liposome formulation. Using PEGylated liposomes decreased liposome uptake by A2780 and A2780 R cells compared to PEG-free formulations, and lowered the effect of positive charge of Ru on cellular uptake. However, PEGylated liposomes are highly beneficial for *in vivo* applications uses as mentioned in the introduction. Actually, finding a compromise between uptake and clearance from the blood stream is not easy; based on the results reported in this chapter 4 mol% PEG in the liposome formulation seems good enough to obtain liposome uptake, in agreement with literature data advocating for ~5 mol% of PEG groups for *in vivo* applications.[40-41]

Cytotoxicity data are not yet complete and suffer from poor statistics. However, initial data disclosed in this work are promising, since liposomes functionalized with ruthenium, either PEGylated or non-PEGylated, showed low dark cytotoxicity against HepG2, A2780 and A2780R cancer cell lines. The poor dark toxicity seems as an advantage for photoactivated chemotherapy (PACT); because in PACT it is the difference in the dark toxicity and the light cytotoxicity that needs to be maximized. In addition high phototoxicity was obtained against HepG2 cells using blue light irradiation (452 nm). Phototoxicity data on A2780 and A2780R cells are not available yet due to technical problems in the experimental setup used to irradiate cancer cells. Light cytotoxicity was only measured for one ruthenium complex supported on PEG-free liposomes and one type of cancer cells, and these experiments should be performed for the other complexes as well, supported on PEGylated liposomes, and for other cancer cell types. Several critical parameters need to be better controlled or changed in future experiments. For example, the irradiation condition was not optimal, since during irradiation of one well the other wells were not kept in the presence of CO_2. Although irradiation time was not too long, the absence of CO_2 might also cause cell death. In addition, the drug exposure time for HepG2 cells was very short (30 min) and may not be representative for what happens *in vivo*. Longer drug exposure times should be investigated to see if different cytotoxicities after light irradiation are observed.

As stated by the cellular uptake results, considering the too high detection limit of ICP-OES ruthenium uptake could not be measured using this technique. In absence of the more sensitive ICP-MS apparatus in the laboratory a fluorescent lipid, NBD-PC, was

included in the liposomes to measure the uptake of the Ru-functionalized liposomes by fluorescence spectroscopy. The fluorescence of the NBD-PC lipid, however, was quenched in presence of ruthenium within the same bilayer membrane, as proven for complex [**1**]$(PF_6)_2$ on DOPC liposomes. The quenching correction for this formulation, however, cannot be generalized for other liposome formulations, as it may be influenced by the detailed structure of the ruthenium complex, by the nature and charge of the lipid, and/or by the presence of PEG groups. Thus, quenching measurements should be performed for each liposome formulation to obtain reliable cell uptake data. In addition, it may be possible that fluorescence quenching in the cellular environment is different from quenching in PBS buffer, as the liposome bilayer might be modified upon entering the cell. Finally, uptake results based on the fluorescence of the NBD-PC lipid would only be correlated to ruthenium uptake if the Ru-S bond is stable and holds the metal complex at the surface of the lipid bilayer in the dark in the cell environment. In this ideal case, cellular uptake of the fluorescently labeled, Ru-functionalized liposomes would indeed mean that the ruthenium prodrug is also taken up by the cells, and that fluorescence data can be interpreted as Ru uptake, after quenching corrections. The thermal stability at 4 °C of the Ru-S bond on DOPC liposomes was good for complex [**3**]$(PF_6)_2$, but such stability cannot be generalized to other complexes, and it should also be proven at 37 °C and in the buffer:medium solution used to incubate the cells. Overall, uptake data based on the method outlined above are only indicative, and a better measurement of ruthenium uptake would be achieved using a more sensitive and reliable method such as ICP-MS.

5.4 Conclusion

Based on the kinetic, uptake, and cytotoxicity data described in this chapter a number of conclusions can be drawn. First, liposomes made of neutral lipids such as DOPC or DMPC are better than negatively charged liposomes based on DOPG or DMPG for supporting the lipophilic Ru polypyridyl complexes [**1**]$(PF_6)_2$ – [**4**]$(PF_6)_2$. The photosubstitution quantum yields are higher, and the uptake of the slightly positively-charged liposomes resulting from neutral liposomes and 5 mol% of dicationic ruthenium complexes is better. Even though the cytotoxicity in the dark is not different from that of liposomes built from negatively charged lipids, their phototoxicity after blue light irradiation on HepG2 cells is higher, probably as a result of a higher uptake. The presence of PEG groups at the surface of the liposomes levels out the difference in

uptake between Ru-functionalized liposomes built from neutral lipids and those based on negatively charged lipids (at least for A2780 and A2780R cells), and also resulted in decreased liposome uptake for both DOPC and DOPG liposomes as a result of the steric hindrance of the PEG groups.

The DOPC and DOPG PEGylated liposomes with or without ruthenium were taken up by A2780 and A2780 R cells in 1 h treatment. The uptake seemed poorly affected by the nature of the ruthenium complexes for both cell lines. However, due to the quenching of fluorescence of NBD-PC by the nearby ruthenium complexes, the uptake results based on fluorescence data cannot strictly be interpreted quantitatively. Dark cytotoxicity results showed that DOPC and DOPG PEGylated liposomes functionalized with any of the four ruthenium complexes [**1**]$(PF_6)_2$ – [**4**]$(PF_6)_2$ were poorly toxic against A2780, or A2780 R cells after 6 hour incubation, and that no difference in toxicity was observed between formulations. On the other hand, cell survival after light irradiation of HepG2 cells treated with non-PEGylated DMPC or DMPG liposomes were lower than that of cells kept in the dark, whether ruthenium (as complex [**1**]$(PF_6)_2$) was present or not.

Overall, liposomes functionalized with polypyridyl ruthenium complexes such as [**1**]$(PF_6)_2$ are promising light-activatable anticancer prodrugs as they are stable in the dark, taken up by cancer cells, poorly toxic in the dark, and more toxic after visible light irradiation. Light toxicity data suggest that light, ruthenium (as complex [**1**]$(PF_6)_2$), and lipids, may be combined in a cancer cell to lead to cell death. However, it is not yet proven that such phototoxicity is related to the photosubstitution reaction that can be measured in a UV-vis cell or in an NMR tube. More studies will be needed to conclude on that, in particular, more data are needed with better statistics, the influence of the structure of the ruthenium complex on the phototoxicity should be assessed, as well as the influence of *e.g.* oxygen concentration, irradiation intensity, or irradiation time on phototoxicity must be determined. Finally, in order to conclude on the potential interest of Ru-functionalized liposomes in anticancer therapy, IC_{50} values in the dark and after light irradiation are needed, as well as dark and light toxicity data on healthy cells and in *in vivo* models of cancer.

5.5 Experimental

5.5.1. Materials and methods

Pymi,[42] [Ru(terpy)(pymi)Cl]PF_6,[42] [Ru(terpy)(bpy)Cl]Cl,[43] ligand **6**,[44] ligand **5**,[36] and ([**1**]$(PF_6)_2$)[45] were synthesized according to literature procedures. Cholesterol, dicyclohexylcarboiimide (DCC), 4-N,N-dimethylaminopyridine (DMAP), $AgBF_4$, and $AgPF_6$ were bought from Sigma-Aldrich. 1,2-dimyristoyl-*sn*-glycero-3-phosphocholine (DMPC), 1,2-dimyristoyl-*sn*-glycero-3-phospho-(1'-rac-glycerol) sodium salt (DMPG), and 1-acyl-2-{12-[(7-nitro-2-1,3-benzoxadiazol-4-yl)amino]dodecanoyl}-*sn*-glycero-3-phosphocholine (NBD-PC), were purchased from Avanti Polar Lipids. 1,2-dioleoyl-*sn*-glycero-3-phosphocholine (DOPC), 1,2-dioleoyl-*sn*-glycero-3-phospho-(1'-rac-glycerol) sodium salt (DOPG), and 1,2-distearoyl-*sn*-glycero-3-phosphoethanolamine-N-[amino(polyethylene glycol)-2000] ammonium salt (DSPG-2KPEG), were bought from Lipoid. All lipids were stored at −20 °C. Syntheses of the metal complexes were performed in the absence of light and under argon. Pierce™ BCA Protein Assay was purchased as a kit from Thermo Scientific (product #23227). Cell Proliferation Reagent WST-1 was purchased as a kit from Roche Diagnostics (product #05015944001). All media, buffers and sterile plastics used for *in vitro* experiments were purchased from SPL Life Sciences or SARSTEDT AG & Co.

^{1}H and ^{13}C NMR spectra were recorded on a Bruker 300 DPX spectrometer at 25 °C (The notations for proton attribution are shown in Figure 5.1). Chemical shifts are indicated in ppm relative to TMS. Characterization of the liposomes (average size and PDI) was done using a Dynamic Light Scattering (DLS) Zetasizer instrument (λ_{irr} = 632 nm) from Malvern. Electrospray mass spectra were recorded on a Finnigan TSQ-quantum instrument by using an electrospray ionization technique (ESI-MS). High resolution mass spectrometry was performed using a Thermo Finnigan LTQ Orbitrap mass spectrometer equipped with an electrospray ion source (ESI) in positive mode (source voltage 3.5 kV, sheath gas flow 10, capillary temperature 275 ºC) with resolution R = 60.000 at *m/z* = 400 (mass range = 150-200) and dioctylphtalate (*m/z* = 391.28428) as "lock mass". Elemental analysis for C, H, N, and S was performed on a Perkin-Elmer 2400 series II analyzer. UV-vis spectra were obtained on a Varian Cary 50 UV-vis spectrometer. The irradiation setup was a LOT 1000 W Xenon arc lamp, fitted with a 400FH90-50 Andover standard cutoff filter and an Andover 450FS10-50 (λ_e=452 nm, $\Delta\lambda_{1/2}$=8.9 nm) interference filter. Photon fluxes of the irradiation setup was measured using the ferrioxalate actinometer.[46] Tecan M1000 PRO plate reader was used for fluorescence or absorbance measurement of multi-well plates for *in vitro* experiments. The ruthenium concentration after uptake was measured by

inductively coupled plasma atomic emission spectroscopy (ICP-OES) on a Varian VISTA-MPX spectrometer. A Beckman Optima™ L-90K Ultracentrifuge machine was used for ultracentrifugation experiments.

5.5.2. Synthesis

Compound **7**. Cholesterol (200 mg, 0.52 mmol) and N-acetyl-L-methionine (100 mg, 0.52 mmol) were dissolved in anhydrous benzene (10 mL) under argon atmosphere. DCC (140 mg, 0.68 mmol) and DMAP (2 mg, 0.02 mmol, 3%) were added and the mixture was stirred vigorously for 12 hours, after which the solution was filtered to remove insoluble materials. The solvent was evaporated under vacuum by rotary evaporation. The crude product was purified by column chromatography on silica gel (petroleum ether/EtOAc 70:30). The solvents were evaporated by rotary evaporation at 30 ºC, and compound **7** was obtained as a white sticky solid. Yield: 50% (150 mg, 0.26 mmol). ^{1}H NMR (300 MHz, $CDCl_3$) δ 6.13 (m, J= 8,18 Hz, 1H, δ), 5.38 (m, J= 4,09 Hz, 1H, 6), 4.70-4.64 (m, 3H, 3, γ), 3.44 (m, 1H, NH), 2.33 (m, 2H, β), 2.10 (s, 3H, α), 2.03 (s, 2H, 4). ^{13}C NMR (75 MHz, $CDCl_3$) δ 171.70 (Cθ), 169.96 (Cε), 139.30 (C5), 123.18 (C6), 75.65 (C3), 56.79, 56.24, 51.90 (Cγ), 50.11, 39.81, 39.62, 38.07 (Cβ), 36.98, 36.68, 36.29, 33.73, 32.22, 32.01, 31.93 (Cα), 30.05, 28.33, 28.12, 27.82, 27.79, 25.60, 24.93, 23.93, 23.36, 22.93, 21.14 (C4), 19.42, 18.83, 15.67, 11.96. ES MS *m/z* (calc): 560.1 (560.4, $[M+H]^+$), 369.2 (369.4, [M-(acetyl-L-methionine)]$^+$). Elemental analysis (%) for $C_{34}H_{57}NO_3S.H_2O$: (calc); C 70.66, H 10.30, N 2.43, S 5.54; (found); C 70.45, H 9.99, N 2.99, S 5.46.

General procedure for the synthesis of [**2**]$(PF_6)_2$, [**3**]$(PF_6)_2$, or [**4**]$(PF_6)_2$. [Ru(terpy)(N-N)(Cl)](Cl) (0.1 mmol), thioether-cholesterol ligand **6** or **7** (0.15 mmol), and $AgBF_4$ (0.2 mmol) were dissolved in acetone (30 mL). The reaction mixture was refluxed overnight for 24 h in the dark, then it was filtered hot over celite, and the solvent was removed by rotary evaporator under reduced pressure. The product was purified by column chromatography on silica gel (acetone/H_2O/sat. aq. KPF_6 (100:10:1.5) or (80:20:4)). The acetone was removed from the collected fractions under vacuum, upon which the product precipitated as an orange solid. The product was filtered, washed with water and dried under vacuum for at least 4 h.

[**2**]$(PF_6)_2$. Yield: 52%. ^{1}H NMR (300 MHz, δ in $CDCl_3$) 9.72 (d, J = 5.3 Hz, 1H, A6), 8.55 (m, J = 8.2 Hz, 3H, A3 + T3'), 8.41 (d, J = 7.9 Hz, 2H, T3), 8.34 (d, J = 8.0 Hz, 1H, B3), 8.27 – 8.14 (m, 2H, A4 + T4'), 8.03 – 7.85 (m, 3H, A5 + T4), 7.74 (t, 1H, B4), 7.68 (d, J = 5.0 Hz, 2H, T6), 7.36 (m, 2H, B5 + B6), 7.16 (m, 2H, T5), 5.30 (d, J = 4.8 Hz, 1H, 6), 3.75 (t, J = 6.6 Hz, 2H, ζ), 3.64 – 3.37 (m, 10H, α + β + γ + δ + ε), 3.13 (s, 1H, 3), 2.40 – 0.75

(m, 47H), 0.67 (s, 3H). ^{13}C NMR (75 MHz, δ in $CDCl_3$) 157.67 + 157.01 + 156.31 + 156.29 (B2+ A2 + T2 + T2'), 153.18 (T6), 151.95 (A6), 149.80 (B6) , 140.86 (5),139.09 (T4), 138.56 +138.37 (B4 + A4), 137.56 (T4'), 128.91 (T5), 128.35 (A5), 127.87 (B5), 125.16 (T3), 124.85 (A3), 124.48 (T3'), 124.03 (B3), 121.86 (6), 79.56 (3), 70.88 + 70.35 + 70.30 + 67.52 + 67.30 (α + β + γ + δ + ε), 56.86, 56.28, 50.26, 42.44, 39.88, 39.64, 39.22, 37.28, 36.97, 36.31, 35.91, 34.47, 32.06, 32.01, 29.82, 28.35, 28.13, 24.42, 23.97, 22.95, 22.69, 21.19, 19.53, 18.85, 15.04, 12.00. UV-vis: λ_{max} (ε in $L \cdot mol^{-1} \cdot cm^{-1}$) in $CHCl_3$: 457 nm (6100). ES MS *m/z* exp (calc): 519.7 (519.4, $[M-2PF_6]^{2+}$). Elemental analysis for $C_{59}H_{79}F_{12}N_5O_3P_2RuS$: (calc); C, 53.31; H, 5.99; N, 5.27; S, 2.41. (Found); C, 53.34; H, 6.22; N, 5.15; S 2.41.

[**3**]$(PF_6)_2$. Yield: 28%. ^{1}H NMR (300 MHz, acetone-d_6) δ 9.98 (d, J= 7.5 Hz, 1H, 6A), 8.95 (m, 3H, 3T',3A), 8.78(d, J= 7,5 Hz, 2H, T6), 8.71(d, J= 7,5 Hz, 1H, 6B), 8.56-8.47 (m, 2H, T4',4A), 8.23-8.13 (m, 3H, T5, 5A), 8.04-8.00 (m, 3H, T3, 5B), 7.57-7.54 (m, 3H, 3B, T4), 7.31 (m, 1H, 4B), 7.17 (d, J= 7,5, 1H, δ), 5.35 (m, 1H, 6), 4.45-4.42 (m, 2H, γ, 3). ^{13}C NMR (75 MHz, acetone-d_6) δ 171.21 (θ), 170.47 (ε), 159.01, 158.43, 157.79, 157.67, 154.43, 154.41, 153.35, 151.01, 140.40 (5), 139.99, 139.95, 139.24, 139.19, 138.05, 129.60, 129.56, 128.90, 128.25, 126.06, 125.68, 125.35, 124.84, 123.46 (6), 75.67 (3), 57.57, 57.06, 51.32 (γ), 51.01, 43.11, 40.61, 40.26, 38.68 (β), 37.66, 37.33, 36.96, 36.59, 32.70 (α), 32.59, 31.12, 30.61, 28.69, 28.35, 24.92, 24.53, 23.07, 22.83, 21.74 (4), 19.65, 19.14, 14.04, 12.23. UV-vis: λ_{max} in nm (ε in $L \cdot mol^{-1} \cdot cm^{-1}$) in $CHCl_3$: 460 nm (8310). ES MS *m/z* (calc): 1195.9 (1195.4, $[M-PF_6]^+$), 525.7 (525.2, $[M-2PF_6]^{2+}$). HRMS *m/z* (calc): 525.23715 (525.23685, $[M-2PF_6]^{2+}$).

[**4**]$(PF_6)_2$. Yield: 34%. ^{1}H NMR (300 MHz, acetone-d6) δ 10.04-10.02 (d, J = 7.3 Hz, 1H, 6Py), δ 9.09 (s, 1H, i), δ 8.69 (d, J=6.8 Hz, 3H, T6 +3Py), 8.59 (d, J = 8.1 Hz, 2H, T3'+T5'), 8.53 (t, J = 7.7 Hz, 1H, 4Py), 8.39 – 8.16 (m, 4H, 5T, 5Py, T4'), 8.08 (dd, J = 11.6, 5.4 Hz, 2H, T3), 7.81 – 7.62 (t, J = 8.1 Hz, 2H, T4), 7.14 (t, J = 8.2, 2H, p-Ph + δ), 7.00 (t, J = 7.8 Hz, 2H, o-Ph), 6.00 – 5.87 (d, 7.2 Hz, 2H, m-Ph), 5.34 (s, 1H, 6), 4.43 (d, J = 8.5 Hz, 2H, γ + 3), 3.62 – 3.44 (m, 1H, ε) 2.24 (s, 2H, β), 1.83 (s, 5H), 1.52 (d, J = 12.3 Hz, 5H), 1.00 (s, 4H), 0.94 (d, J = 6.5 Hz, 3H), 0.86 (dd, J = 6.6, 1.0 Hz, 6H), 0.71 (s, 3H). ^{13}C NMR (75 MHz, acetone-d6) δ 205.31 (θ), 170.34 (ε), 170.07 (i), 158.07 (T2 or T2' or 2Py), 156.77 (T2 or T2' or 2Py), 154.18 (T3), 153.02, 147.13 (T2 or T2' or 2Py), 139.47 (T5), 138.05 (4Py), 136.77 (T4'), 131.44 (3Py), 129.57 (5Py), 129.23 (o-Ph), 129.06 (4T), 129.01, 128.01 (p-Ph, 124.85 (6T), 123.73 (3T'), 122.65 (6), 119.95 (m-Ph), 74.82 (ε), 56.72, 56.21, 50.40 (3), 50.15, 42.26, 39.76, 39.42, 37.84, 36.81, 36.48, 36.12, 35.77, 33.80, 31.85, 31.75, 30.53, 29.79, 29.53, 29.27, 29.02, 28.76, 28.63, 28.50, 28.25, 28.07, 27.87, 27.51, 24.09, 23.69, 22.50, 22.25, 22.00, 20.90, 18.81, 18.31, 14.47, 13.46, 11.39.

ES MS *m/z* (calc): 1221.5 (1221.45, $[M - PF_6]^+$), 707.0 (707.1, $[M - 2PF_6 - \text{cholesteryl}]^+$), 538.3 (538.2, $[M-2PF_6)]^{2+}$). UV-vis: λ_{max} (ε in $L \cdot mol^{-1} \cdot cm^{-1}$) in acetone: 475 nm (10300). Elemental analysis for $C_{61}H_{78}F_{12}N_6O_3P_2RuS$: calc: C 53.62, H 5.75, N 6.15, S 2.35 found: C 54.44, H 5.66, N 5.98, S 1.45.

5.5.3. Liposome preparation

Stock solutions of phospholipids (5.0×10^{-3} M in $CHCl_3$ or $CHCl_3$:CH_3OH (4:1)) and of ruthenium complexes [**1**]$(PF_6)_2$ – [**4**]$(PF_6)_2$ (5.0×10^{-4} M in $CHCl_3$) were prepared and stored at −20 °C. The stock solutions were mixed in proportions corresponding to the desired liposome formulation. The solvents of the lipid mixture were evaporated to form a lipid film at the bottom of a glass tube. Traces of solvent were removed under high vacuum for at least 1 h. Each sample was then hydrated with the desired buffer (PBS: Phosphate Buffered Saline or chloride-free phosphate buffer: 10 mM of phosphates, I = 50 mM, pH = 6.97) at 50 °C. The bulk lipid concentration in each sample was 2.50 mM and the ruthenium concentration for ruthenium-functionalized liposomes was 0.125 mM. Each sample was put through at least 10 freeze/thaw cycles (from liquid nitrogen to 50 °C) until a clear solution was obtained. The liposome solution was then extruded at least 11 times at 50 °C using the Avanti Polar Lipids mini-extruder fitted with a 200 nm pore diameter Whatman polycarbonate filter. After extrusion, the samples were characterized by Dynamic Light Scattering (DLS) at 25 °C to determine the average diameter (130 – 140 nm in general). The samples were stored in the dark at 4 °C if not used right away.

5.5.4. Light irradiation of liposome samples and UV-vis experiments

A liposome sample (1.5 mL) containing phospholipids (2.5 mM) and a ruthenium complex [**1**]$(PF_6)_2$, [**2**]$(PF_6)_2$, [**3**]$(PF_6)_2$, or [**4**]$(PF_6)_2$ (5 mol%, 0.125 mM) in a phosphate buffer solution, (I=50 mM, pH=7.0) was placed into a UV-vis cell. 1.5 mL of the phosphate buffer solution was added to the cuvette. The final concentrations of the lipid and of the ruthenium complex in the cuvette were 1.3 mM and 0.065 mM, respectively. The UV-vis spectrum of the sample was first measured in the dark. Then the sample was irradiated at 452 nm using the beam of a LOT 1000 W Xenon arc lamp filtered by an Andover bandpath filter, and directed into an 2.5 mm diameter optical fiber bundle bringing the light inside the spectrophotometer, vertically to the cuvette axis, *i.e*, perpendicular to the horizontal optical axis of the spectrophotometer (see Appendix I, Figure AI.1*)*. The UV-vis spectrum of the sample was measured every 3 minutes during irradiation while stirring at 25 °C or 37 °C. The irradiation time varied between 2 and 6 h (depending to the kinetics of the reaction) to reach the photochemical steady state. The concentrations in *[RuSRR']* ([**1**]$^{2+}$ to [**4**]$^{2+}$) was

determined by deconvolution knowing the extinction coefficients of both RuSRR' and $RuOH_2$ species (see Appendix I and V). The evolution of ln($[RuSRR']/[Ru]_{tot}$) was plotted as a function of irradiation time, and from the slope S of the plot $-k_{\varphi}$ at λ_e=452 nm was determined for each sample. Knowing the photon flux and probability of photon absorption $1-10^{-3Ae}$, where A_e is the absorbance of the solution at the excitation wavelength λ_e, the number of moles of photons Q absorbed at time t by RuSRR' since t_e=0 was calculated. Plotting $n_{RuSRR'}$ *vs.* Q gave a straight line in each case. The slope of this plot directly corresponds to the quantum yield of the photosubstitution reaction (see Appendix I, Section AI.3.2).

5.5.5. Stability of the ruthenium-sulfur bond in PBS in the dark

7 mL of a DOPC:DSPE-PEG2K (98:2) liposome sample containing 5 mol% of complex [**3**]$(PF_6)_2$ was prepared in PBS (total lipid bulk concentration: 2.5 mM, $[Ru]_{tot}$=0.125 mM). 6.5 mL of this liposome solution was diluted with 6.5 mL of PBS (final lipid concentration: 1.25 mM, $[Ru]_{tot}$=0.065 mM). 4 mL fractions of this solution were subjected to ultracentrifugation (speed = 40,000 rpm, RCF = 100,000 g, T = 20 °C, time = 2 h) at different times (1 day, 3 days, and 7 days) after sample preparation. The ruthenium content of the supernatant and of the liposome sample before ultracentrifugation were measured by ICP-OES (sample was prepared as described in Appendix V).

5.5.6. Cell lines and culture conditions

The human ovarian carcinoma cell line A2780 and its cisplatin resistant analogue A2780R were grown as a monolayer at 37 °C in 7% CO_2 atmosphere, and were maintained in a continuous logarithm culture in Dulbecco's Modified Eagle Medium (DMEM) containing phenol red completed with 10% Fetal Calf Serum (FCS), penicillin/ streptomycin (100 units/ml, 0.1 mg/ml, respectively), and Glutamax (2 mM). This medium will be further referred to as 'DMEM (+FCS, +P/S, +ph. red). Human liver hepatocellular carcinoma cells HepG2 were grown in HepaRG medium at 37 °C in 5% CO_2 atmosphere.

5.5.7. Cellular uptake assay

For cellular uptake experiments, liposome solutions containing 4% NBD-PC were prepared in PBS as described in section 5.5.3. 24-well plates were seeded with A2780 or A2780 R cells at 5.0×10^4 cells/well. Typically, a plate seeded with cells was pre-incubated for 3 days (A2780) or 2 days (A2780 R) at 37 °C in 7% CO_2 atmosphere until ~100% confluence was reached. At the day of cells treatment with the liposome sample, cell culture medium in the wells was replaced with fresh medium DMEM (−FCS, + P/S, +ph. red) at 37 °C 1.5 h

before treatment. 800 µL of liposome solution in PBS was diluted with 500 µL of DMEM (−FCS, + P/S, +ph. red) (total lipid bulk concentration =1.5 mM, ruthenium concentration = 0.075 mM). Before incubating the cells with liposome solutions, the medium was aspirated from each well. Then the cells were exposed to 300 µL of liposome-DMEM solution for 1 h at 37 °C in 7% CO_2 atmosphere in the dark. Control wells were filled with 300 µL of a PBS:DMEM (−FCS, +PS, +ph. red) (8:5) mixture. After 1 h liposome exposure, the liposome solution was removed and the cells were gently washed once with 1 mL PBS. Then 500 µL of PBS was added to each well and the fluorescence of NBD-PC lipids taken up by the cells was read with a fluorescence spectrophotometer (λ_{exc} = 460 nm, λ_{em} = 534 nm). PBS was then removed, 500 µL of 0.2 M NaOH was added to each well, and the plate was rocked at r.t. for 1 hour to lyse the cells. The cell lysis was either used directly in a BCA protein determination assay or stored at −20 °C for later use in a BCA protein assay (see section5.5.8). To determine the cellular uptake, the fluorescence measurement F for each well, due to the NBD-PC lipids, were divided by the absorbance values A_{prot} obtained from the BCA assay. Finally, F/A_{prot} for each well was divided by $(F/A_{prot})_{\mathrm{ctrl}}$ of the well containing cells that were not treated with liposomes, to obtain the "fold increase of F/A" as compared to the control (normalized values for control = 1 or 100%). The obtained value represents the cellular uptake of each liposome sample. The ruthenium content of the cell lysis was measured by ICP-OES as well (see Appendix AV.2 for the sample preparation protocol).

5.5.8. BCA protein determination assay

Protein determination was done using the BCA (bicinchoninic acid) protein determination assay (PierceTM BCA Protein Assay Kit, Thermo Scientific). For this assay, a working reagent was prepared from reagents included in the BCA protein assay kit: Reagent A: Bicinchoninic acid and tartrate in an alkaline carbonate buffer solution. Reagent B: 4% $CuSO_4.5H_2O$ (aqueous solution). The working reagent was prepared by mixing reagent A and B in a volumetric ratio of 50:1. For the BCA assay, a 96-well plate was filled with 200 µL of the working reagent in each well. 25 µL of the cell lysis (in 0.2 M NaOH) after cytotoxicity or uptake experiment (cells were killed in NaOH 0.2 M) was mixed with the working reagent in the corresponding wells of the 96-wells plate. As a control, 25 µL of Milli-Q was added to 200 µL working reagent. After addition, the working reagent and the cell lysis solutions were properly mixed. The plate was then protected from light and incubated at 37 °C and 7% CO_2 for 30 minutes, and the absorbance (A_{prot}) of each well in the plate was then measured at 562 nm using a Tecan M1000 PRO plate reader.

5.5.9. Confocal microscopy measurements

Confocal microscopy culture dishes (cover glass bottom dish, 35×10 mm, gamma irradiated, SPL Life Sciences) were incubated with fibronectin (0.0005%; 1:200 dilution, Sigma-Aldrich, F1141) in 0.9% NaCl for 1-2 h at 37 °C. Typically, 300 µL is used per well in an 8-well plate. This volume should be corrected for well surface if wells of other dimensions are used. HepG2 cells (3.2×10^5) were seeded on confocal microscopy culture dishes (on the cover glass only) and grown for 24 h in HepaRG medium (volume = 2.5 mL)at 37 °C in an atmosphere of 5% CO_2. Before incubation with liposomes (containing 5% fluorescent NBD-PC lipid) in order to do fluorescence measurements, the growth medium was aspirated and replaced with 1.5 mL of fresh William's E Medium containing penicillin/streptomycin (100 unit/mL and 0.1 mg/mL, respectively) and glutamax (2mM), equilibrated at 37 °C. Next, 500 µL of the liposome suspension (lipid concentration = 0.50 mM in chloride-free phosphate buffer:PBS (1:4), ruthenium 0 or 5 mol%) was added to the culture dish. The cells were incubated for 1 h at 37 °C in an atmosphere of 5% CO_2 and 95% air. Before confocal microscopy, cells were washed 3 times with 2 mL PBS equilibrated at 37 °C. 2 mL of PBS was added to the culture dish and the cells were imaged by confocal microscopy (Leica Microsystems, SP2 confocal microscope, 63 times oil immersion objective).

5.5.10. Dark cytotoxicity assay

A2780 or A2780 R cells were seeded at 5.0×10^4 cells/well and grown in 500 µL DMEM (+FCS, +PS, + ph. red) in 24 well-plates. No cells were seeded in well F4. The plates were pre-incubated for either 2 days (A2780 R) or 3 days (A2780) at 37 °C in 7% CO_2 atmosphere until ~100% confluence was reached. The medium was refreshed 1.5 h before exposure of the cells with liposome solutions. Liposome samples (without NBD-PC) were prepared in PBS before the start of the experiment as described in section 5.5.3 and diluted with DMEM as described in section 5.5.7. Total lipid concentration and ruthenium concentration were 1.5 mM and 0.075 mM, respectively. The medium was removed from the wells and 300 µL of liposome stock solution at r.t. was added in each well. The cells were then incubated for 6 h at 37 °C and 7% CO_2 in the dark. After incubation, the supernatant was removed from the cell wells. The cells were washed once with 1 mL of PBS at r.t and 500 µL of fresh DMEM (+FCS, +PS, −ph. red) was added to each well. The cells were then incubated for 24 h at 37 °C and 7% CO_2, before measuring cell metabolic activity using the WST-1 assay (see section 5.5.11).

5.5.11. WST-1 assay

WST-1 is a colorimetric assay for the quantification of cellular proliferation and cytotoxicity. As mentioned in section 5.5.10, the cells were incubated in a drug-free medium for 24 h prior to perform WST-1 assay. After 24 h, the medium was replaced with 250 µL of fresh DMEM (+FCS, +PS, −ph. red). Well F4 was filled with 250 µL of DMEM (+FCS, +PS, −ph. red) to be used as a control (no cells in this well). Absorbance of each well was read at 450 nm to check for possible absorption of ruthenium in the absorption range of WST-1 (420 to 480 nm), but the ruthenium absorption was negligible and almost equal to that of wells that contained no ruthenium. The plate was then incubated for 15 minutes at 37 °C and 7% CO_2, after which the cell proliferation reagent WST-1 (1/10 of the medium volume: 25 µL) was added to each well. The WST-1 and the medium in the wells were properly mixed and the plate was incubated for 60 minutes at 37 °C and 7% CO_2. After incubation, the absorbance of the solution in each well was read again at 450 nm. The supernatant was then removed and cells were washed once with 1 mL of PBS at r.t. Cells were then lysed by adding 500 µL of 0.2 M NaOH to each well and the plate was incubated for 1 h at r.t. while rocking. The protein content of the cell lysis was then determined by a BCA assay (see section 5.5.8). WST-1 cell proliferation results W' were corrected by subtracting the absorbance value found for the control well (F4) W'_{ctrl}. The values $W=W'-W'_{ctrl}$ were then divided by the protein absorption data A_{prot} obtained from a BCA assay, to give the metabolic activity of the cells per well W/A_{prot}. By dividing the metabolic activity found for each well, by the metabolic activity of the control wells $(W/A_{prot})_{ctrl}$ (no liposomes), the values for metabolic activity (cell survival) were normalized with respect to control (no liposomes), which was set to be 100% cell survival.

5.5.12. Light cytotoxicity assay

HepG2 cells were seeded at 2.5×10^4 cells/well and grown in 500 µL HepaRG (+FCS, +PS, + ph. red) in 24 well-plates. Control wells contained no cells. The plate was pre-incubated for 2 days at 37 °C in 5% CO_2 atmosphere. The medium was refreshed 1.5 h before exposure of the cells to the liposomes. Liposome samples (without NBD-PC) in chloride-free phosphate before (800 µL) were diluted with PBS (1200 µL). Total lipid concentration and ruthenium concentration were 2 mM and 0.1 mM, respectively. The medium was removed from the wells and 200 µL of liposome stock solution at r.t. was added to each well in the dark and the cells were incubated for 30 min at 37 °C and 5% CO_2 in the dark. After 30 min liposome exposure, the liposome suspension was removed; the cells were washed once with 500 µL of PBS (37 °C) in the dark. Subsequently, 300 µL of HepaRG was added per well and the plate was incubated in the dark at 37 °C in 5% CO_2 atmosphere

for 15 min. The plate was placed on a custom-built heated aluminum pad (37 °C, measured with a thermocouple, set temp water bath = 58.5 °C) and irradiated at 452 nm for 15 min per well (light toxicity) in an otherwise dark room (dark toxicity). The filter was cooled with pellets of dry ice (irradiation parameters: incident spot diameter = 2.3 cm; power = 69 mW, light intensity: 17 $mW \cdot cm^{-2}$). After irradiation, 200 µL of HepaRG medium was added to each well of both plates and the cells were incubated for 1 day prior to perform WST-1 assay. The metabolic activity of the cells was determined as described in section 5.5.11 and compared with the metabolic activity of the HepG2 cells which were exposed to the same liposome samples (for 30 min) but kept in the dark during the irradiation time (dark cytotoxicity).

5.6 References

[1] A. Levina, A. Mitra, P. A. Lay, *Metallomics* **2009**, *1*, 458-470.
[2] A. Bergamo, C. Gaiddon, J. H. M. Schellens, J. H. Beijnen, G. Sava, *J. Inorg. Biochem.* **2012**, *106*, 90-99.
[3] W. Han Ang, P. J. Dyson, *Eur. J. Inorg. Chem.* **2006**, *2006*, 4003-4018.
[4] V. Pierroz, T. Joshi, A. Leonidova, C. Mari, J. Schur, I. Ott, L. Spiccia, S. Ferrari, G. Gasser, *J. Am. Chem. Soc.* **2012**, *134*, 20376-20387.
[5] D. Ossipov, S. Gohil, J. Chattopadhyaya, *J. Am. Chem. Soc.* **2002**, *124*, 13416-13433.
[6] I. Kostova, *Curr. Med. Chem.* **2006**, *13*, 1085-1107.
[7] G. Stochel, A. Wanat, E. Kuliś, Z. Stasicka, *Coord. Chem. Rev.* **1998**, *171*, 203-220.
[8] N. J. Farrer, L. Salassa, P. J. Sadler, *Dalton Trans.* **2009**, 10690-10701.
[9] M. C. DeRosa, R. J. Crutchley, *Coord. Chem. Rev.* **2002**, *233–234*, 351-371.
[10] A. Juzeniene, Q. Peng, J. Moan, *Photochem. Photobiol. Sci.* **2007**, *6*, 1234-1245.
[11] B. S. Howerton, D. K. Heidary, E. C. Glazer, *J. Am. Chem. Soc.* **2012**, *134*, 8324-8327.
[12] M. J. Clarke, *Coord. Chem. Rev.* **2003**, *236*, 207.
[13] R. E. Goldbach, I. Rodriguez-Garcia, J. H. van Lenthe, M. A. Siegler, S. Bonnet, *Chem. Eur. J.* **2011**, *17*, 9924-9929.
[14] D. Peer, J. M. Karp, S. Hong, O. C. FaroKhzad, R. Margalit, R. Langer, *Nat. Nanotechnol.* **2007**, *2*, 751-760.
[15] T. L. Andresen, S. S. Jensen, K. Jorgensen, *Prog. Lipid Res.* **2005**, *44*, 68-97.
[16] M. Frasconi, Z. C. Liu, J. Y. Lei, Y. L. Wu, E. Strekalova, D. Malin, M. W. Ambrogio, X. Q. Chen, Y. Y. Botros, V. L. Cryns, J. P. Sauvage, J. F. Stoddart, *J. Am. Chem. Soc.* **2013**, *135*, 11603-11613.
[17] Gregoria.G, E. J. Wills, C. P. Swain, A. S. Tavill, *Lancet* **1974**, *1*, 1313-1316.
[18] K. W. Ferrara, M. A. Borden, H. Zhang, *Acc. Chem. Res.* **2009**, *42*, 881-892.
[19] A. K. Giddam, M. Zaman, M. Skwarczynski, I. Toth, *Nanomed.* **2012**, *7*, 1877-1893.
[20] G. Sharma, S. Anabousi, C. Ehrhardt, M. Kumar, *J. Drug Target.* **2006**, *14*, 301-310.
[21] Y. Malam, M. Loizidou, A. M. Seifalian, *Trends Pharmacol. Sci.* **2009**, *30*, 592-599.
[22] M. L. Immordino, F. Dosio, L. Cattel, *Int. J. Nanomedicine* **2006**, *1*, 297-315.
[23] M. C. Woodle, M. S. Newman, J. A. Cohen, *J. Drug Target.* **1994**, *2*, 397-403.
[24] A. S. L. Derycke, P. A. M. de Witte, *Adv. Drug Delivery Rev.* **2004**, *56*, 17-30.

[25] T. M. Allen, C. Hansen, F. Martin, C. Redemann, A. Yauyoung, *Biochim. Biophys. Acta* **1991**, *1066*, 29-36.
[26] T. M. Allen, A. Chonn, *FEBS Lett.* **1987**, *223*, 42-46.
[27] N. Maurer, D. B. Fenske, P. R. Cullis, *Expert Opin. Biol. Ther.* **2001**, *1*, 923-947.
[28] D. C. Drummond, C. O. Noble, M. E. Hayes, J. W. Park, D. B. Kirpotin, *J. Pharm. Sci.* **2008**, *97*, 4696-4740.
[29] W. T. Al-Jamal, K. Kostarelos, *Acc. Chem. Res.* **2011**, *44*, 1094-1104.
[30] K. Djanashvili, T. L. M. ten Hagen, R. Blange, D. Schipper, J. A. Peters, G. A. Koning, *Bioorg. Med. Chem.* **2011**, *19*, 1123-1130.
[31] G. N. Kaluderovic, A. Dietrich, H. Kommera, J. Kuntsche, K. Maeder, T. Mueller, R. Paschke, *Eur. J. Med. Chem.* **2012**, *54*, 567-572.
[32] H. Chen, R. C. MacDonald, S. Li, N. L. Krett, S. T. Rosen, T. V. O'Halloran, *J. Am. Chem. Soc.* **2006**, *128*, 13348-13349.
[33] K. J. Harrington, G. Rowlinson-Busza, K. N. Syrigos, R. G. Vile, P. S. Uster, A. M. Peters, J. S. W. Stewart, *Clin. Cancer Res.* **2000**, *6*, 4939-4949.
[34] L. Simeone, G. Mangiapia, G. Vitiello, C. Irace, A. Colonna, O. Ortona, D. Montesarchio, L. Paduano, *Bioconjug. Chem.* **2012**, *23*, 758-770.
[35] G. Mangiapia, G. D'Errico, L. Simeone, C. Irace, A. Radulescu, A. Di Pascale, A. Colonna, D. Montesarchio, L. Paduano, *Biomaterials* **2012**, *33*, 3770-3782.
[36] S. Bonnet, B. Limburg, J. D. Meeldijk, R. J. M. K. Gebbink, J. A. Killian, *J. Am. Chem. Soc.* **2010**, *133*, 252-261.
[37] M. Kvasnica, M. Budesinsky, J. Swaczynova, V. Pouzar, L. Kohout, *Bioorg. Med. Chem.* **2008**, *16*, 3704-3713.
[38] P. K. Smith, R. I. Krohn, G. T. Hermanson, A. K. Mallia, F. H. Gartner, M. D. Provenzano, E. K. Fujimoto, N. M. Goeke, B. J. Olson, D. C. Klenk, *Anal. Biochem.* **1985**, *150*, 76-85.
[39] M. Ishiyama, M. Shiga, K. Sasamoto, M. Mizoguchi, P. G. He, *Chem. Pharm. Bull.* **1993**, *41*, 1118-1122.
[40] D. D. Lasic, D. Needham, *Chem. Rev.* **1995**, *95*, 2601-2628.
[41] S. M. Moghimi, J. Szebeni, *Prog. Lipid Res.* **2003**, *42*, 463-478.
[42] A. C. G. Hotze, J. A. Faiz, N. Mourtzis, G. I. Pascu, P. R. A. Webber, G. J. Clarkson, K. Yannakopoulou, Z. Pikramenou, M. J. Hannon, *Dalton Trans.* **2006**, 3025-3034.
[43] K. J. Takeuchi, M. S. Thompson, D. W. Pipes, T. J. Meyer, *Inorg. Chem.* **1984**, *23*, 1845-1851.
[44] A. Bahreman, B. Limburg, M. A. Siegler, R. Koning, A. J. Koster, S. Bonnet, *Chem. Eur. J.* **2012**, *18*, 10271-10280.
[45] S. Bonnet, B. Limburg, J. D. Meeldijk, R. J. M. K. Gebbink, J. A. Killian, *J. Am. Chem. Soc.* **2011**, *133*, 252-261.
[46] J. G. P. Calvert, J. N., *Chemical actinometer for the determination of ultraviolet light intensities. In Photochemistry*,Wiley and Sons, New York, **1967**; 780.